Dalton Transactions

ROYAL SOCIETY OF CHEMISTRY

PAPER

View Article Online
View Journal | View Issue

Cite this: *Dalton Trans.*, 2025, **54**, 10441

Heterobimetallic unsaturated silicon clusters (siliconoids) with transition metal-expanded scaffolds†

Luisa Giarrana,[a] Nadine E. Poitiers,[a] Alida Stürmer,[a] Michael Zimmer,[a] Volker Huch,[a] Bernd Morgenstern[b] and David Scheschkewitz *[a]

We report a heterobimetallical unsaturated silicon cluster (siliconoid) with a formally anionic group 9 metal vertex (Ir) in close contact to the lithium counter-cation, thus constituting a rare example of transition metal–lithium interactions. The anionic cluster is obtained by reductive chloride elimination from the corresponding neutral siliconoid complex of iridium(I) chloride with lithium/naphthalene. The previously exohedral transition metal center is fully incorporated into the siliconoid cluster scaffold giving rise to an irida-heterosiliconoid reminiscent of the corresponding homonuclear Si_7 species. Despite the formal negative charge at the iridium center, the nucleophilic site is on one of the adjacent silicon vertices judging from the reactivity toward group 4 metallocene dichlorides, Cp_2MCl_2 (M = Zr, Hf). Under elimination of LiCl, the Cp_2MCl moieties in the heterobimetallic products are installed as pending functionalities under retention of the literally uncompromised iridasiliconoid core.

Received 14th May 2025,
Accepted 12th June 2025

DOI: 10.1039/d5dt01135c

rsc.li/dalton

Introduction

Heterobimetallic species have been receiving growing attention over the last decades due to their unique electronic and catalytic properties. Mixed metallic compounds are frequently used as catalysts, for instance in the production of H_2 in the context of energy storage,[1a] as enzyme surrogates in water oxidation[1b] or in (m)ethanol fuel cells.[1c,d] In Fischer–Tropsch chemistry, bimetallic phases[1e] and – increasingly – heterobimetallic nanoparticles are competent heterogenous catalysts.[1f] Numerous bimetallic main group-transition metal complexes have been reported for their activity in homogenous catalysis,[2] among them neutral compounds such as **I**[3a] (N_2 reduction) and anionic derivatives such as **II** (CO_2 derivatization).[3b] Late first and second row transition metals readily form metal-element bonds to E_n ligands (*e.g.* E = group 13 to 15 atom), but the controlled implementation of a second or third transition metal center remains a challenge, especially if different to the first.[4]

Due to the low electronegativity of the constituting elements, main group metalloid clusters, such as Zintl anions,[5] represent competent ligand systems for late transition metals and thus considerable potential in homogenous catalysis.[5] Especially germanium and tin-based Zintl anions[6] and – more recently – their silicon congeners have been employed as extraordinarily electron-rich ligands towards transition metal centers.[7] More specifically, Zintl clusters with either metal vertices (*e.g.* **III**, Fig. 1)[8] or endohedral metal centers (*e.g.* **IV**)[9] have been described, along with dimeric clusters such as **V**.[7a] Even multimetallic cluster species have been reported by the groups of Goicoechea and Sevov: the straightforward addition of a second transition metal to a rhodium-germanium cluster **VI** leads to the formation of **VII**[10] (Fig. 1) or a Rh–Ir intermetallic cluster **VIII**.[11] With the neutral rhodium species **VI**, the first example of a homogeneous catalyst derived from Zintl anions was disclosed with considerable activity in alkene hydrogenation and H/D exchange.[10]

As we proposed based on the isolation of lithiated derivatives, unsaturated silicon clusters (siliconoids)[12] as otherwise neutral molecular species are conceptually related to Zintl anions through the formal replacement of negative charges by covalently bonded substituents.[13] Accordingly, the availability of nucleophilic anionic siliconoids provided access to the first transition metal-substituted derivatives: a *ligato*-lithiated Si_6 siliconoid served as a precursor for X-type ligation toward $M(Cp)_2Cl$ (M = Zr, Hf).[12g] In contrast, the realization of L-type coordination required the grafting of a tetrylene

[a]*Krupp-Chair in Inorganic and General Chemistry, Saarland University, Campus C4.1 Saarbrücken, 66123 Saarbrücken, Germany.*
E-mail: david.scheschkewitz@uni-saarland.de
[b]*Service Center X-Ray Diffraction, Saarland University Campus Saarbrücken C4.1, 66123 Saarbrücken, Germany*

†Electronic supplementary information (ESI) available. CCDC 2447272, 2447286 and 2447266. For ESI and crystallographic data in CIF or other electronic format see DOI: https://doi.org/10.1039/d5dt01135c

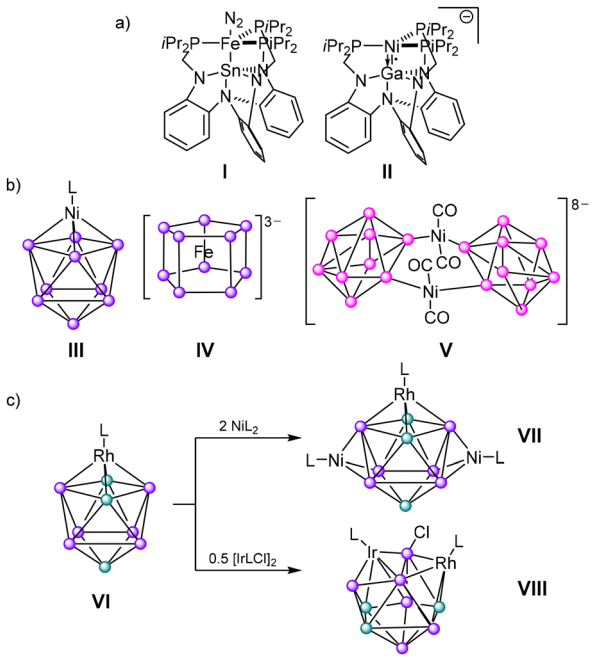

Fig. 1 (a) Selected examples of heterobimetallic complexes with main group elements and (b) transition metal-incorporating Zintl anions of the main group elements (c) heteromultimetallic Zintl-type complexes (● = Ge, ● = Ge-Hyp, ● = Si; L = cyclooctadienyl, Hyp = tris(trimethylsilyl)silyl).

side-arm in the *ligato* position. The resulting globally neutral metallasiliconoid **1** (Scheme 1),[13g,h] however, exhibits only partial incorporation of the group 9 metal into the cluster scaffold due to the cage-opening chlorine transfer from the transition metal. Nonetheless, **1** proved to be competitively active and selective as the catalyst of the isomerization of 1-hexene to 2-hexene.

Herein, we report the first complete inclusion reactions of any transition metal as hetero-vertices of siliconoids using a reductive elimination approach. The reaction of **1** gives rise to a 7-vertex iridasiliconoid reminiscent of the neutral Si_7 derivative. The product shows close contacts between the transition metal centers and the lithium counter-cation, further highlighting the conceptual relationship between siliconoids and Zintl anions. Finally, we demonstrate that heterobimetallic complexes with group 4 metals are readily obtained by reaction

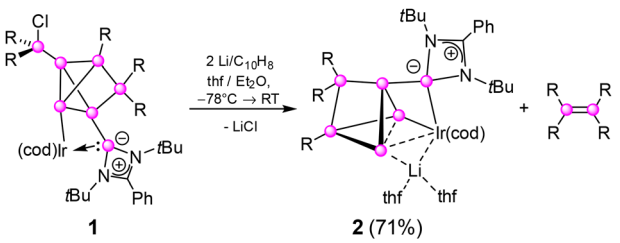

Scheme 1 Synthesis of Si_6Ir-Li **2** by reduction of **1**[12h] with $Li/C_{10}H_8$ (● = Si; R = 2,4,6-triisopropylphenyl, cod = 1,5-cyclooctadiene).

of the anionic clusters with the appropriate metallocene dichlorides.

Results and discussion

We anticipated that the reductive elimination of chloride from the incompletely metal-incorporated siliconoid **1** may either prompt the reintegration of its pending chlorosilyl group into the cluster framework or its complete cleavage. Both eventualities could in principle result in additional metal-cluster interactions and hence prompt the desired complete incorporation of the metal center into the cluster core. Indeed, reaction of **1** with lithium/naphthalene in thf led to the complete cleavage of the exohedral Tip_2SiCl-group to yield a new product **2** in 71% isolated yield (Scheme 1). The lithium salt **2** was fully characterized by X-ray diffraction on single crystals, UV/vis spectroscopy and multinuclear NMR spectroscopy.

The product mixture shows the characteristic ^{29}Si NMR signal of tetrakis(2,4,6-triisopropylphenyl)disilene at 52.8 ppm,[14] which is apparently formed as a systematic by-product that can however be separated by crystallization. The distribution of the remaining ^{29}Si NMR chemical shifts of **2** is akin to that of Si_6- and Si_7 siliconoids.[12a,c,e,g] According to the 2D $^{29}Si/^{1}H$ correlation of the isolated product, the deshielded signal at 152.8 ppm is assigned to the $SiTip_2$ unit and the most shielded resonances at −184.0 and −226.3 ppm to the Ir-bonded unsubstituted silicon vertices. One further highfield signal at −103.2 ppm can be attributed to the vertex carrying the amidinato silylene, which in turn gives rise to a signal at 36.0 ppm, slightly downfield-shifted compared to the precursor (**1**: $\delta^{29}Si$ 32.9 ppm).[12h] The SiTip vertex resonates at 108.2 ppm and thus at unusually low field. Most notably, the major ^{7}Li NMR signal of **2** is significantly downfield-shifted to 5.99 ppm. A minor broad signal at 1.12 ppm likely belongs to a different coordination mode of the Li counter-ion that however, does not affect the coordination and the chemical shifts of the remaining nuclei.

Single crystals of **2** were obtained from hexane in 71% yield and the molecular structure in the solid state was confirmed by X-ray diffraction (Fig. 2a). The unit cell contains two molecules of **2** in the asymmetric unit with slightly differing bonding values. In the following, the arithmetic mean values will be discussed (see ESI Table S2† for exact values). The cleavage of the exohedral silyl group in **1** indeed resulted in the full incorporation of the Ir(cod) center into a distorted benzpolarene motif in **2**. The term benzpolarene was recently introduced by our group to refer to the highly polarized, tetracyclic global minimum isomer of benzene, in analogy to benzvalene as another prominent isomer of benzene.[12e] The amidinato silylene sidearm in **2** completes the coordination sphere at Ir1, while Li1 assumes a bridging position across the Si2–Ir1 bond.

The anionic iridasiliconoid **2** is therefore best described as a heteroanalogue of the doubly bridged propellane motif of the Si_7 scaffolds **IX** and **X**, although with some noteworthy differences (Fig. 2b).[12d] While in **IX** and **X**, the "upper" three

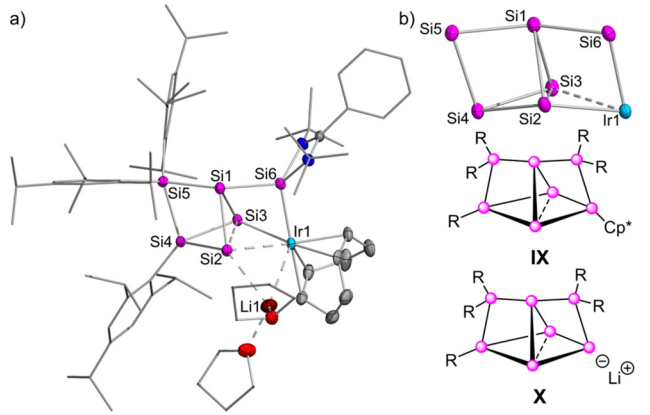

Fig. 2 (a) Molecular structure of iridasiliconoid as contact ion pair **2** in the solid state. The inverted structure (1 − *x*, 1 − *y*, 1 − *z*) is displayed for consistent visualization. Hydrogen atoms omitted for clarity. Thermal ellipsoids at 50% probability. Arithmetic mean values of selected bond lengths [Å] and angles [°]: Ir1–Li1 2.880(8), Si2–Li1 2.611(8), Ir1–Si2 2.641(1), Ir1–Si6 2.344(1), Ir1–Si3 2.411(1), Si2–Si3 2.475(2), Si1–Si6 2.285(2), Si1–Si5 2.321(2), Si1–Si2 2.327(2), Si1–Si3 2.423(2), Si2–Si4 2.388(2), Si3–Si4 2.331(2), Si4–Si5 2.402(2); Si6–Ir1–Li1 122.7(2), Si3–Ir1–Li1 107.1(2), Si3–Si2–Li1 113.9(2), Si2–Ir1–Li1 56.3(2), Si6–Ir1–Si3 69.2(4), Si5–Si1–Si6 149.9(7); (b) Central cluster motif in comparison with 7-vertex clusters **IX** and **X** (● = Si, R = 2,4,6-triisopropylphenyl, Cp* = C_5Me_5).

silicon atoms are almost linear (**IX**: 173.8°, **X**: 174.0°) giving rise for a seesaw coordination environment, the apical silicon atom Si1 of the central triangular motif of **2** is canted away from the Si5–Si6 vector towards Si2, the basal silicon atom connected to the lithium counter-cation (Si5–Si1–Si6 149.9 (7)°). This is presumably a consequence of the tetravalency of this vertex (whereas Si3 is formally trivalent), which implies a more electron-precise bonding situation with considerably shorter bonds. Concomitantly, Si1 acquires a much more pronounced hemispheroidal coordination environment (**2**: ϕ = 0.5542, **IX**: ϕ = −0.0390, **X**: ϕ = −0.0994).[13k] For a tetracoordinate atom, the hemispheroidality parameter ϕ describes the deviation of the "naked" silicon vertex from a reference plane, defined by the three bonded atoms, for which the sum of bond angles is closest to 360°, in comparison to a fourth substituent, which is set to be a negative value as per convention.[13k] If ϕ results in a negative value, a tetrahedral coordination is suggested, whereas a positive value indicates a hemispheroidal coordination environment of the vertex in question.

The distance between the unsubstituted vertices in **2** (Si2–Si3 2.475(2) Å) is remarkably shortened compared to homonuclear Si_6 and Si_7 siliconoids.[12a,c,e,g] The metal-silicon bond due to the L-type coordination by the silylene side arm (Si6–Ir1 2.344(1) Å) is significantly shorter than the X-type interaction with the *nudo*-vertex Si3 (Si3–Ir1 2.411(1) Å). These values are in line with previously reported silicon-iridium single bonds (2.245 Å–2.574 Å).[15] The pronounced lengthening of the third silicon-iridium contact (Ir1–Si2 2.641(1) Å) can be attributed to the bridging by the lithium counteraction in the sense of an unprecedented agostic 3c2e Ir–Si–Li interaction. In fact, only very few Ir–M (M = alkali metal) contact ion pairs have been crystallographically characterized.[16] Despite its bridging nature, the Ir1–Li1 distance of 2.880(8) Å in **2** is in good agreement with the reported Ir···Li distances in a diphenyliridate (2.882/2.886 Å).[17] The distance between Si2···Li1 (2.611(8) Å) in **2** is well within the range of further reported Si···Li siliconoid distances (2.56–2.77 Å).[12c–e]

The longest wavelength absorption in the UV/vis spectrum of **2** at λ_{max} = 543 nm is slightly blue-shifted compared to the starting material **1** (λ_{max} = 576 nm) but red-shifted in contrast to previously reported *ligato*-substituted siliconoids (λ_{max} = 364 to 521 nm).[12c,e,g] The TD-DFT calculated value at $\lambda_{max,calc}$ = 528 nm (PBE0/DEF2-TZVPP level of theory)[18] confirms the assignment to the HOMO → LUMO transition (78% contribution, see ESI† for further details). Besides, an additional intense absorption band at λ = 425 nm agrees well with calculated transitions at 418 nm (HOMO−3 → LUMO 35%, HOMO−2 → LUMO 39%) and 430 nm (HOMO → LUMO + 3 78%) (ESI Table S7†).

We probed the reactivity of Si_6Ir-Li **2** towards Me_3SiCl and Me_3SnCl, as representative common electrophiles. The components of the reaction mixture, however, could not be isolated nor identified with certainty. To explore the application of anionic Si_6Ir-Li **2** as a precursor for the grafting of a second transition metal center, we then investigated the reaction with group 4 metallocene dichlorides as electrophilic substrates (Scheme 2) since $ZrCp_2Cl_2$ and $HfCp_2Cl_2$ were shown to readily undergo clean salt metathesis reactions in the case of homonuclear siliconoids and as well as electron-precise silicon species.[12g,20] The reactions of **2** with Cp_2MCl_2 (M = Zr, Hf) in benzene at room temperature yielded the corresponding substituted siliconoids **3a**,**b** in isolated yields of 14% and 32%, respectively. Interestingly, **3a** proved to be much less stable than **3b** leading to as yet unidentified decomposition products during work-up. The yields are furthermore compromised by the competing formation of an unidentified side product, which could be due to the elimination of CpLi according to residual ^{1}H and ^{13}C NMR signals in the spectra of **3a**/**3b** at 5.869/5.810 ppm and 114.32/112.85 ppm, respectively (ESI†).[19] Attempts to detect CpLi by ^{7}Li NMR, however, remained unsuccessful.

The NMR spectra of **3a**,**b** show very similar signal patterns. The ^{29}Si NMR signals were assigned based on 2D ^{29}Si/^{1}H NMR

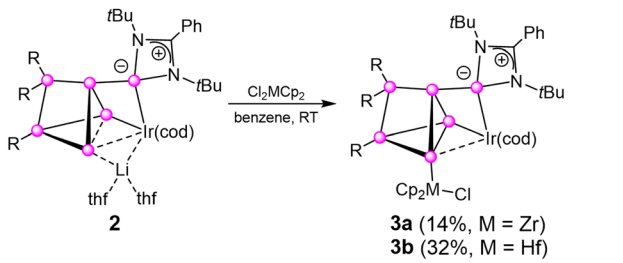

Scheme 2 Synthesis of group 4 metallocenyl-substituted iridasiliconoids **3a**,**b** from **2** and Cl_2MCp_2 (M = Zr (**3a**), Hf (**3b**); ● = Si; R = 2,4,6-triisopropylphenyl; cod = 1,5-cyclooctadiene).

correlation spectra. The signals of the $SiTip_2$ unit (**3a**: 73.8 ppm, **3b**: 75.9 ppm) are significantly upfield-shifted with a $\Delta\delta$ of about 75 ppm compared to the starting material (**2**: 149.3 ppm). Similar highfield-shifts are observed for the SiTip units, assigned based on the cross-peaks in the aromatic region (**2**: 108.2 ppm, **3a**: 73.5 ppm, **3b**: 68.1 ppm). The resonance attributed to the Si atom of the pending N-heterocyclic silylene (**3a**: 30.5 ppm, **3b**: 29.9 ppm) is found in the same range as the corresponding signals of the precursors (**1**: 32.9 ppm, **2**: 36.0 ppm) suggesting that the environment of the coordinated Ir-cod moiety is mostly preserved. The most downfield-shifted resonance compared to **2** is the signal assigned to the Si–M atom (**2**: −226.3 ppm, **3a**: −40.9 ppm, **3b**: −36.6 ppm). The two remaining highfield signals (**3a**: −77.9/−131.9 ppm, **3b**: −90.4/−131.1 ppm) correlate to the unsubstituted silicon atoms (Si1, Si3) but are somewhat more deshielded than in the starting material (**2**: −103.2/−184.0 ppm).

Compared to the starting material **2**, the longest wavelength absorptions in the UV/vis spectra of **3a**,**b** are considerably red-shifted from λ_{max} = 551 nm (**2**) to 601 nm (**3a**, Zr) and 647 nm (**3b**, Hf) indicating a significantly smaller HOMO–LUMO gap.

Single crystals of both **3a** (14%) and **3b** (32%) were obtained overnight from concentrated hexane solutions at −26 °C (**3a**) and room temperature (**3b**) (Fig. 3). X-ray diffraction analysis confirmed the molecular structures in the solid state with formation of bonds between the group 4 metal M (M = Zr, Hf) and Si2 rather than Ir1, possibly because of the higher stability of Si–M bonds[21] compared to bimetallic transition metal bonds as well as the larger differences in electronegativity (Pauling values Si 1.90, Zr 1.33, Hf 1.3, Ir 2.20).[22] The elongated distance between Si2 and Ir1 (Fig. 3, **3a**: 2.726(1) Å, **3b**: 2.748(1) Å) compared to **2** (2. 641(1) Å) suggests a somewhat weaker interaction in line with the presence of the additional Si2–M bond. Consequently, the Si2–Si3 bond (**2**: 2.475(2) Å) is shortened to the length of a typical Si–Si single bond (2.30–2.40 Å, **3a**: 2.388(1) Å, **3b**: 2.390(2) Å).[21b] The Si2–M bond lengths (**3a**: 2.744(9) Å, **3b**: 2.723(1) Å) are on the shorter end of reported Si-M (M = Zr, Hf) single bonds (Si–Zr = 2.7429–2.924 Å, Si–Hf = 2.729–2.939 Å).[12g,21] Comparable bond distances were reported for tris(trimethylsilyl) hafnium derivatives by Rheingold, Geib and Tilley, (d_{Si-Hf} = 2.729 Å/ 2.748 Å)[21a,b] and for a zirconocenecyclosilane by Marschner and coworkers (2.743 Å).[21c] Table 1 compares pertinent structural and spectroscopic data of heterobimetallic siliconoids **2**, **3a** and **3b**.

As in the case of **2**, the seesaw coordination at Si1 is strongly distorted to a hemispheroidal environment (**3a**: ϕ = 0.7148, **3b**: ϕ = 0.7206). The more covalent bonding of the Si–M bond in **3a** and **3b** gives rise to even more acute Si5–Si1–Si6

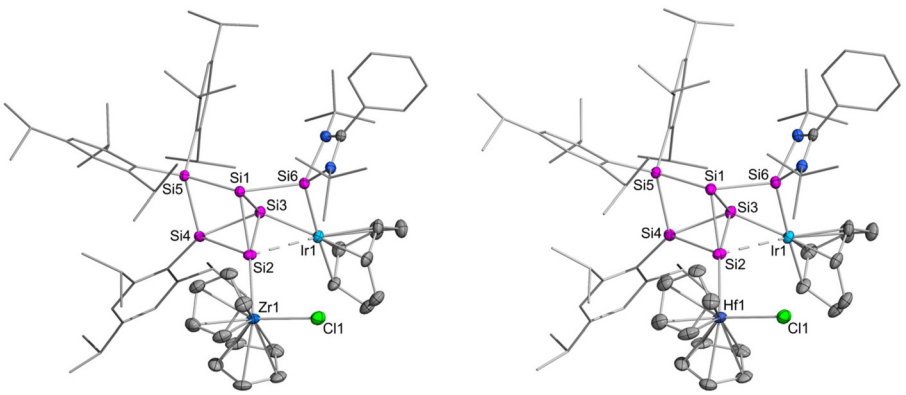

Fig. 3 Molecular structures of heterobimetallic siliconoids **3a** (left) and **3b** (right) in the solid state. The inverted structure (1 − *x*, 1 − *y*, 1 − *z*) is displayed for consistent visualization. Hydrogen atoms are omitted for clarity. Thermal ellipsoids are set at 50% probability. Selected bond lengths [Å] and angles [°]: (a) Ir1–Si2 2.726(1), Ir1–Si3 2.345(9), Ir1–Si6 2.319(9), Zr1–Si2 2.744(9), Zr1–Cl1 2.452(9), Si2–Si3 2.388(1), Si1–Si3 2.495(1), Si1–Si2 2.336(1); Si6–Ir1–Si3 71.0(3), Si6–Ir1–Si2 78.3(3), Si3–Ir1–Si2 55.6(3), Ir1–Si2–Zr1 112.4(3), Cl1–Zr1–Si2 103.0(3), Si3–Si4–Si2 60.2(4), Si5–Si4–Si2 101.0(4) Si5–Si1–Si6 136.4(2); (b) Ir1–Si2 2.748(1), Ir1–Si3 2.345(1), Ir1–Si6 2.318(2), Hf1–Si2 2.723(1), Hf1–Cl1 2.420(1), Si2–Si3 2.390(2), Si1–Si3 2.492(2), Si1–Si2 2.338(2); Si6–Ir1–Si3 70.9(5), Si6–Ir1–Si2 78.1(4), Si3–Ir1–Si2 55.3(4), Ir1–Si2–Hf1 113.9(5), Cl1–Hf1–Si2 100.8(4), Si3–Si4–Si2 57.5 (5), Si5–Si4–Si2 101.1(6), Si5–Si1–Si6 135.9(7).

Table 1 Selected analytical data of **2** and **3a**,**b**. Literature data of precursor **1** for comparison[12h]

Compound	δ^{29}Si NH*Si* [ppm]	δ^{29}Si unsubstituted *Si* [ppm]	*d* (Si–Si, unsubstituted) [Å]	*d*(Si2–M) [Å]	◁ Si5–Si1–Si6 [°]
Si_7Ir **1**	32.9	−125.6/−128.8	2.305(2)/2.548(2)	2.305(2)	—
Si_6Ir-Li **2**	36.0	−184.0/−226.3	2.475(2)	2.658(1)	149.9(7)
Si_6Ir-Zr **3a**	73.5	−77.9/−131.9	2.388(12)/2.495(1)	Si2···Ir1 2.726(1)/Si2–Zr1 2.744(9)	136.4(2)
Si_6Ir-Hf **3b**	68.1	−90.4/−131.1	2.390(2)/2.494(2)	Si2···Ir1 2.748(1)/Si2–Hf1 2.723(1)	135.9(7)

angles than in **2** (**3a**: 136.4(2)°, **3b**: 135.9(7)°, **2**: 149.9(7)°) and the Si_7 siliconoids **IX** and **X** (Fig. 2, **IX**: 173.8°, **X**: 174.0°).[12a] Although the Cl1–M1–Si2 angle (**3a**: 103.0(3), **3b**: 100.8(4)°) is more acute than expected, an initially suspected Ir–Cl interaction is unlikely given the rather long distances (Ir···Cl: 4.5206(9) Å (**3a**), 4.478(2) Å (**3b**)).

Conclusions

In conclusion, we report on the isolation and full characterization of the first heterobimetallic siliconoid with fully incorporated transition metal vertex. The contact ion pair **2** comprising the anionic iridasiliconoid and the lithium countercation resembles the corresponding Si_7 siliconoid species. Reactions of **2** with Cp_2MCl_2 (M = Zr and Hf) results in the heterobimetallic siliconoids **3a** and **3b** in which the group 4 metal moiety is exohedrally attached to the silicon vertex in α-position to iridium while the irida-incorporated heterosiliconoid scaffold is preserved in principle.

Author contributions

L. Giarrana, N. E. Poitiers and A. Stürmer performed the synthetic work and data analysis, L. Giarrana, N. E. Poitiers and D. Scheschkewitz designed the study, D. Scheschkewitz acquired the funding; V. Huch and B. Morgenstern carried out the X-ray diffraction studies, M. Zimmer did the solid state and VT NMR measurements, L. Giarrana performed the DFT calculations, L. Giarrana and D. Scheschkewitz wrote the manuscript.

Conflicts of interest

There are no conflicts of interest to declare.

Data availability

All data associated with this manuscript are available in the ESI.† Crystallographic data for **2**, **3a** and **3b** have been deposited at the CCDC (2447272, 2447286 and 2447266†) and can be obtained from **https://www.ccdc.cam.ac.uk/structures**.

Acknowledgements

Funding by the Deutsche Forschungsgemeinschaft (DFG SCHE 906/4-4) is gratefully acknowledged. Instrumentation and technical assistance for this work were provided by the Service Center X-ray Diffraction, with financial support from Saarland University and German Science Foundation (project number INST 256/506-1). The authors thank Dr. Diego Andrada and Prof. Stella Stopkowicz for access to their computational clusters.

References

1 (*a*) M. R. DuBois and D. L. DuBois, The roles of the first and second coordination spheres in the design of molecular catalysts for H_2 production and oxidation, *Chem. Soc. Rev.*, 2009, **38**, 62; (*b*) R. Brimblecombe, G. F. Swiegers, G. C. Dismukes and L. Spiccia, Sustained water oxidation photocatalysis by a bioinspired manganese cluster, *Angew. Chem., Int. Ed.*, 2008, **47**, 7335; (*c*) E. Antolini, Catalysts for direct ethanol fuel cells, *J. Power Sources*, 2007, **170**, 1; (*d*) S. Song, W. Zhou, Z. Liang, R. Cai, G. Sun, Q. Xin, V. Stergiopoulos and P. Tsiakaras, The effect of methanol and ethanol cross-over on the performance of PtRu/C-based anode DAFCs, *Appl. Catal., B*, 2005, **55**, 65; (*e*) B. H. Davis, Fischer–Tropsch synthesis: Overview of reactor development and future potentialities, *Top. Catal.*, 2005, **32**, 143; (*f*) U. Pal, J. F. Sanchez Ramirez, H. B. Liu, A. Medina and J. A. Ascencio, Synthesis and structure determination of bimetallic Au/Cu nanoparticles, *Appl. Phys. A*, 2004, **79**, 79.

2 Selection of reviews on heterometallic complexes in homogeneous catalysis: (*a*) P. Buchwalter, J. Rosé and P. Braunstein, Multimetallic catalysis based on heterometallic complexes and clusters, *Chem. Rev.*, 2015, **115**, 28; (*b*) W. Xu, M. Li, L. Qiao and J. Xie, Recent advances of dinuclear nickel-and palladium-complexes in homogeneous catalysis, *Chem. Commun.*, 2020, **56**, 8524; (*c*) S. A. Laneman and G. G. Stanley, Homogeneous Bimetallic Hydroformylation Catalysis - Two Metals Are Better Than One, in *Adv. in Chem*, Amercian Chemical Society, 1992, ch. 24, vol. 230, pp. 349–366; (*d*) R. G. Fernando, C. D. Gasery, M. D. Moulis, G. G. Stanley, M. Iglesias, E. Sola, L. A. Oro, I. Dutta, G. Sengupta, J. K. Bera, M. J. Page, D. B. Walker, B. A. Messerle, E. Bodio, M. Picquet, P. Le Gendre, M. Garland, L. Gan, D. Jennings, J. Laureanti and A. K. Jones, in *Homo- and heterobimetallic complexes in catalysis*, ed. P. Kalck, Springer International Publishing, Switzerland, 1st edn, 2016; (*e*) R. M. Haak, S. J. Wezenberg and A. W. Kleij, Cooperative multimetallic catalysis using metallosalens, *Chem. Commun.*, 2010, **46**, 2713.

3 (*a*) M. J. Dorantes, J. T. Moore, E. Bill, B. Mienert and C. C. Lu, Bimetallic iron–tin catalyst for N_2 to NH_3 and a silyldiazenido model intermediate, *Chem. Commun.*, 2020, **56**, 11030; (*b*) M. V. Vollmer, R. C. Cammarota and C. C. Lu, Reductive Disproportionation of CO2 Mediated by Bimetallic Nickelate(–I)/Group 13 Complexes, *Eur. J. Inorg. Chem.*, 2019, 2140.

4 (*a*) E. Zintl and A. Harder, Polyplumbide, Polystannide und ihr Übergang in Metallphasen, *Z. Phys. Chem. Abt. A*, 1931, **154a**, 47; (*b*) T. F. Fässler, in *Zintl Ions: Principles and Recent Developments*, Struct. Bonding, Springer-Verlag, Berlin, Heidelberg, 2011; (*c*) S. Scharfe, F. Kraus, S. Stegmeier, A. Schier and T. F. Fässler, Zintl ions, cage compounds, and intermetalloid clusters of group 14 and group 15 elements, *Angew. Chem., Int. Ed.*, 2011, **50**, 3630;

(*d*) R. J. Wilson, D. Weinert and S. Dehnen, Recent developments in Zintl cluster chemistry, *Dalton Trans.*, 2018, **47**, 14861.

5 (*a*) M. T. Whited, Pincer-supported metal/main-group bonds as platforms for cooperative transformations, *Dalton Trans.*, 2021, **50**, 16443; (*b*) M. T. Whited, Metal–ligand multiple bonds as frustrated Lewis pairs for C–H functionalization, *Beilstein J. Org. Chem.*, 2012, **8**, 1554; (*c*) M. T. Whited and B. L. H. Taylor, Metal/organosilicon complexes: structure, reactivity, and considerations for catalysis, *Comments Inorg. Chem.*, 2020, **40**, 217.

6 (*a*) W. T. Pennington, R. C. Haushalter and B. W. Eichhorn, Synthesis and structure of closo-$Sn_9Cr(CO)_3^{4-}$: The first member in a new class of polyhedral clusters, *J. Am. Chem. Soc.*, 1988, **110**, 8704; (*b*) J. M. Goicoechea and S. C. Sevov, Organozinc Derivatives of Deltahedral Zintl Ions: Synthesis and Characterization of *closo*-$[E_9Zn(C_6H_5)]^{3-}$ (E = Si, Ge, Sn, Pb), *Organometallics*, 2006, **25**, 4530; (*c*) E. N. Esenturk, J. Fettinger and B. Eichhorn, Synthesis and characterization of the $[Ni_6Ge_{13}(CO)_5]^{4-}$ and $[Ge_9Ni_2(PPh_3)]^{2-}$ Zintl ion clusters, *Polyhedron*, 2006, **25**, 521; (*d*) S. Scharfe, T. F. Fässler, S. Stegmaier, S. D. Hoffmann and K. Ruhland, $[Cu@Sn_9]^{3-}$ and $[Cu@Pb_9]^{3-}$: Intermetalloid Clusters with Endohedral Cu Atoms in Spherical Environments, *Chem. – Eur. J.*, 2008, **14**, 4479; (*e*) N. S. Willeit, V. Hlukhyy and T. F. Fässler, Synthesis, Structure and Catalytic Properties of $Hyp_3[Ge_9Rh]PPh_3$, *Z. Anorg. Allg. Chem.*, 2024, **24**, e202400171.

7 (*a*) S. Joseph, M. Hamberger, F. Mutzbaurer, O. Härtl, M. Meier and N. Korber, Chemistry with Bare Silicon Clusters in Solution: A Transition–Metal Complex of a Polysilicide Anion, *Angew. Chem., Int. Ed.*, 2009, **48**, 8770; (*b*) M. Waibel, F. Kraus, S. Scharfe, B. Wahl and T. F. Fässler, $[(MesCu)_2(\eta^3\text{-}Si_4)]^4$: A mesitylcopper-stabilized tetrasilicide tetraanion, *Angew. Chem., Int. Ed.*, 2010, **49**, 6611; (*c*) D. O. Downing, P. Zavalij and B. W. Eichhorn, The *closo*–$[Sn_9Ir(cod)]^{3-}$ and $[Pb_9Ir(cod)]^{3-}$ Zintl Ions: Isostructural IrI Derivatives of the *nido*,–E_9^{4-} Anions (E = Sn, Pb), *Eur. J. Inorg. Chem.*, 2010, 890; (*d*) F. S. Geitner and T. F. Fässler, Low oxidation state silicon clusters–synthesis and structure of [NHC Dipp Cu $(\eta^4\text{-}Si_9)]^{3-}$, *Chem. Commun.*, 2017, **53**, 12974.

8 J. M. Goicoechea and S. C. Sevov, Deltahedral germanium clusters: insertion of transition-metal atoms and addition of organometallic fragments, *J. Am. Chem. Soc.*, 2006, **128**, 4155.

9 B. Zhou, M. S. Denning, D. L. Kays and J. M. Goicoechea, Synthesis and Isolation of $[Fe@Ge_{10}]^{3-}$: A Pentagonal Prismatic Zintl Ion Cage Encapsulating an Interstitial Iron Atom, *J. Am. Chem. Soc.*, 2009, **131**, 2802.

10 O. P. E. Townrow, C. Chung, S. A. Macgregor, A. S. Weller and J. M. Goicoechea, A neutral heteroatomic zintl cluster for the catalytic hydrogenation of cyclic alkenes, *J. Am. Chem. Soc.*, 2020, **142**, 18330.

11 O. P. E. Townrow, A. S. Weller and J. M. Goicoechea, Controlled cluster expansion at a Zintl cluster surface, *Angew. Chem., Int. Ed.*, 2024, **63**, e202316120.

12 (*a*) K. Abersfelder, A. J. P. White, R. J. F. Berger, H. S. Rzepa and D. Scheschkewitz, A Stable Derivative of the Global Minimum on the Si_6H_6 Potential Energy Surface, *Angew. Chem., Int. Ed.*, 2011, **50**, 7936; (*b*) A. Jana, V. Huch, M. Repisky, R. J. F. Berger and D. Scheschkewitz, Dismutational and global–minimum isomers of heavier 1,4–dimetallatetrasilabenzenes of group 14, *Angew. Chem., Int. Ed.*, 2014, **53**, 3514; (*c*) P. Willmes, K. I. Leszczyńska, Y. Heider, K. Abersfelder, M. Zimmer, V. Huch and D. Scheschkewitz, Isolation and versatile derivatization of an unsaturated anionic silicon cluster (siliconoid), *Angew. Chem., Int. Ed.*, 2016, **55**, 2907; (*d*) K. I. Leszczyńska, V. Huch, C. Präsang, J. Schwabedissen, R. J. F. Berger and D. Scheschkewitz, Atomically precise expansion of unsaturated silicon clusters, *Angew. Chem., Int. Ed.*, 2019, **58**, 5124; (*e*) Y. Heider, N. E. Poitiers, P. Willmes, K. I. Leszczyńska, V. Huch and D. Scheschkewitz, Site-selective functionalization of Si_6R_6 siliconoids, *Chem. Sci.*, 2019, **10**, 4523; (*f*) L. Klemmer, V. Huch, A. Jana and D. Scheschkewitz, An anionic heterosiliconoid with two germanium vertices, *Chem. Commun.*, 2019, **55**, 10100; (*g*) N. E. Poitiers, L. Giarrana, K. I. Leszczyńska, V. Huch, M. Zimmer and D. Scheschkewitz, Indirect and Direct Grafting of Transition Metals to Siliconoids, *Angew. Chem., Int. Ed.*, 2020, **59**, 8532; (*h*) N. E. Poitiers, L. Giarrana, V. Huch, M. Zimmer and D. Scheschkewitz, Exohedral functionalization vs. core expansion of siliconoids with Group 9 metals: catalytic activity in alkene isomerization, *Chem. Sci.*, 2020, **11**, 7782; (*i*) N. E. Poitiers, V. Huch, M. Zimmer and D. Scheschkewitz, Chalcogen-Expanded Unsaturated Silicon Clusters: Thia-, Selena-, and Tellurasiliconoids, *Chem. – Eur. J.*, 2020, **26**, 16599; (*j*) N. E. Poitiers, V. Huch, M. Zimmer and D. Scheschkewitz, Siliconoid Expansion by a Single Germanium Atom through Isolated Intermediates, *Angew. Chem., Int. Ed.*, 2022, **61**, e202205399; (*k*) Y. Heider, P. Willmes, V. Huch, M. Zimmer and D. Scheschkewitz, Boron and phosphorus containing heterosiliconoids: stable p-and n-doped unsaturated silicon clusters, *J. Am. Chem. Soc.*, 2019, **141**, 19498.

13 (*a*) D. Scheschkewitz, A molecular silicon cluster with a "naked" vertex atom, *Angew. Chem., Int. Ed.*, 2005, **44**, 2954; (*b*) M. Moteki, S. Maeda and K. Ohno, Systematic search for isomerization pathways of hexasilabenzene for finding its kinetic stability, *Organometallics*, 2009, **28**, 2218; (*c*) D. Nied, R. Köppe, W. Klopper, H. Schnöckel and F. Breher, *J. Am. Chem. Soc.*, 2010, **132**, 10264; (*d*) K. Abersfelder, A. J. P. White, H. S. Rzepa and D. Scheschkewitz, Synthesis of a Pentasilapropellane. Exploring the Nature of a Stretched Silicon– Silicon Bond in a Nonclassical Molecule, *Science*, 2010, **327**, 564; (*e*) S. Ishida, K. Otsuka, Y. Toma and S. Kyushin, An organosilicon cluster with an octasilacuneane core: a missing silicon cage motif, *Angew. Chem., Int. Ed.*, 2013, **52**, 2507; (*f*) A. Tshurusaki, C. Iizuka, K. Otsuka and S. Kyushin, Cyclopentasilane-fused hexasilabenzvalene, *J. Am. Chem.*

Soc., 2013, **135**, 16340; (*g*) A. Tsurusaki, K. Kamiyama and S. Kyushin, Tetrasilane-Bridged Bicyclo [4.1. 0] heptasil-1 (6)-ene, *J. Am. Chem. Soc.*, 2014, **136**, 12896; (*h*) F. Breher, Stretching bonds in main group element compounds—Borderlines between biradicals and closed-shell species, *Coord. Chem. Rev.*, 2007, **251**, 1007; (*i*) T. Iwamoto and S. Ishida, Silicon compounds with inverted geometry around silicon atoms, *Chem. Lett.*, 2014, **43**, 164; (*j*) S. Kyushin, in *Organosilicon Compounds: Theory and Experiment (Synthesis)*, ed. V. Y. Lee, Academic Press (Elsevier), 2017, vol. 1, ch. 3, pp. 69–144; (*k*) Y. Heider and D. Scheschkewitz, Stable unsaturated silicon clusters (siliconoids), *Dalton Trans.*, 2018, **47**, 7104; (*l*) Y. Heider and D. Scheschkewitz, Molecular silicon clusters, *Chem. Rev.*, 2021, **121**, 9674.

14 (*a*) H. Watanabe, K. Takeuchi, N. Fukawa, M. Kato, M. Goto and Y. Nagai, Air-stable tetrakis (2, 4, 6-triisopropylphenyl) disilene. Direct synthesis of disilene from dihalomonosilane, *Chem. Lett.*, 1987, **16**, 1341; (*b*) H. Watanabe, K. Takeuchi, K. Nakajima, Y. Nagai and M. Goto, The First Preparation of Disilene via Reductive DehaIogenation of 1,2-DichIorodisiIane. The Formation of an Unusual Air-Oxidation Product, 1-Oxa-2-silacyclopent-3-ene Derivative, *Chem. Lett.*, 1988, **17**, 1343.

15 (*a*) S. Kaufmann, S. Schäfer, M. T. Gamer and P. W. Roesky, Reactivity studies of silylene $[PhC(NtBu)_2](C_5Me_5)$ Si–reactions with [M (COD) Cl]$_2$ (M= Rh (i), Ir (i)), S, Se, Te, and BH_3, *Dalton Trans.*, 2017, **46**, 8861; (*b*) M. Stoelzel, C. Präsang, B. Blom and M. Driess, N-heterocyclic silylene (NHSi) rhodium and iridium complexes: synthesis, structure, reactivity, and catalytic ability, *Aust. J. Chem.*, 2013, **66**, 1163; (*c*) M. Aizenberg, J. Ott, C. J. Elsevier and D. Milstein, Rh(I) and Rh(III) silyl PMe3 complexes. Syntheses, reactions and ^{103}Rh NMR spectroscopy, *J. Organomet. Chem.*, 1998, **551**, 81.

16 (*a*) M. Karni, J. Kapp, P. von Ragué Schleyer, Y. Apeloig and Z. Rappoport, in *The Chemistry of Organic Silicon Compounds*, ed. Z. Rappoport and Y. Apeloig, John Wiley & Sons, Chichester, 2001, ch. 1, vol. 3, pp. 1–183; M. Weidenbruch, Chapter 3, pp. 391–428; (*b*) M. Kraftory, M. Kapon and M. Botoshansky, *The Chemistry of Organic Silicon Compounds*, ed. Z. Rappoport and Y. Apeloig, John Wiley & Sons, Chichester, 1998, ch. 5, vol. 2, pp. 181–264.

17 T. Iwasaki, T. Akaiwa, Y. Hirooka, S. Pal, K. Nozaki and N. Kambe, Synthesis of and structural insights into contact ion pair and solvent-separated ion pair diphenyliridate complexes, *Organometallics*, 2020, **39**, 3077.

18 PBE0: (*a*) J. P. Perdew, M. Ernzerhof and K. Burke, Rationale for mixing exact exchange with density functional approximations, *J. Chem. Phys.*, 1996, **105**, 9982; (*b*) C. Adamo and V. Barone, Toward reliable density functional methods without adjustable parameters: The PBE0 model, *J. Chem. Phys.*, 1999, **110**, 6158; (*c*) J. P. Perdew, K. Burke and M. Ernzerhof, Generalized gradient approximation made simple, *Phys. Rev. Lett.*, 1996, **77**, 3865.

19 S. Bachmann, B. Gernert and D. Stalke, Solution structures of alkali metal cyclopentadienides in THF estimated by ECC-DOSY NMR-spectroscopy (incl. software), *Chem. Commun.*, 2016, **52**, 12861.

20 T.-L. Nguyen and D. Scheschkewitz, Activation of a Si=Si Bond by η1-Coordination to a Transition Metal, *J. Am. Chem. Soc.*, 2005, **127**, 10174.

21 (*a*) H.-G. Woo, R. H. Heyn and T. D. Tilley, σ-Bond metathesis reactions for d0 metal-silicon bonds that produce zirconocene and hafnocene hydrosilyl complexes, *J. Am. Chem. Soc.*, 1992, **114**, 5698; (*b*) J. Arnold, D. M. Roddick, T. D. Tilley, A. L. Rheingold and S. J. Geib, Preparation and characterization of tris (trimethylsilyl) silyl and tris (trimethylsilyl) germyl derivatives of zirconium and hafnium. X-ray crystal structures of $(\eta^5\text{-}C_5Me_5)Cl_2HfSi(SiMe_3)_3$ and $(\eta^5\text{-}C_5Me_5)Cl_2HfGe(SiMe_3)_3$, *Inorg. Chem.*, 1988, **27**, 3510; (*c*) R. Fischer, D. Frank, W. Gaderbauer, C. Kayser, C. Mechtler, J. Baumgartner and C. Marschner, α, ω-Oligosilyl Dianions and Their Application in the Synthesis of Homo- and Heterocyclosilanes, *Organometallics*, 2003, **22**, 3723; (*d*) C. Kayser, D. Frank, J. Baumgartner and C. Marschner, Reactions of oligosilyl potassium compounds with Group 4 metallocene dichlorides, *J. Organomet. Chem.*, 2003, **667**, 149; (*e*) Z. Dong, C. R. W. Reinhold, M. Schmidtmann and T. Müller, A Stable Silylene with a σ^2, π- Butadiene Ligand, *J. Am. Chem. Soc.*, 2017, **139**, 7117; (*f*) T.-I. Nguyen and D. Scheschkewitz, Activation of a Si Si Bond by η-Coordination to a Transition Metal, *J. Am. Chem. Soc.*, 2005, **127**, 10174; (*g*) Z. Wu, J. B. Diminnie and Z. Xue, Synthesis and Characterization of Group 4 Amido Silyl Complexes Free of Anionic π-Ligands, *Inorg. Chem.*, 1998, **37**, 6366; (*h*) A. Sauermoser, T. Lainer, G. Glotz, F. Czerny, B. Schweda, R. C. Fischer and M. Haas, Synthesis and Characterization of Methoxylated Oligosilyl Group 4 Metallocenes, *Inorg. Chem.*, 2022, **61**, 14742; (*i*) B. L. L. Reant, D. De Alwis Jayasinghe, A. J. Wooles, S. T. Liddle and D. P. Mills, Comparison of group 4 and thorium M(IV) substituted cyclopentadienyl silanide complexes, *Dalton Trans.*, 2023, **52**, 7635.

22 L. Pauling, *J. Am. Chem. Soc.*, 1947, **69**, 542.